OPTIMAL PROPERTIES OF SURFACE MODIFIED CELLULOSE AS FILLER IN POLYMER COMPOSITES

PETRA SKALKOVÁ,[*] ZUZANA MIČICOVÁ,[*] IVETA PAPUČOVÁ,[*] JANA PAGÁČOVÁ,[*] IVAN LABAJ[*] and BEÁTA PECUŠOVÁ[**]

[*]*Faculty of Industrial Technologies, A. Dubček University of Trenčín, Ivana Krasku 491/30, 020 01 Púchov, Slovak Republic*
[**]*TnUAD of Trenčín, FunGlass – Centre for Functional and Surface Functionalized Glass, Trenčín, Slovak Republic*
✉ *Corresponding author: P. Skalková, petra.skalkova@tnuni.sk*

Received June 11, 2024

The research and development of new materials that are not only functional, but also ecologically acceptable, is a key aspect in many branches of industry. Such materials include elastomeric composites reinforced with alternative fillers such as cellulose. Cellulose is a renewable and biodegradable alternative to traditional fillers used in elastomeric composites. The main disadvantage of this biopolymer is its poor compatibility with the hydrophobic matrix and low mechanical strength. The free hydroxyl groups on the cellulose surface allow for a wide range of surface modifications. In this work, we focused on the chemical modification of cellulose using two different silanes due to their ability to react with the free hydroxyl groups on the surface of cellulose. This work deals with the characterisation of thermal stability of surface modified cellulose used as filler in polymer composites. Cellulose modified in this way was used in the amount of 45 phr as a filler in the preparation of elastomeric composites with natural rubber (NR) matrix. The NR composite filled with surface modified cellulose was characterized by TG/DSC, IR spectroscopy, XRD and scanning electron microscopy.

Keywords: biopolymers, surface modification, polymer composites, silane, thermal stability

INTRODUCTION

Currently, there is great interest in the use of renewable sources of raw materials in the manufacture of environmentally friendly products. Such materials also include natural fibers with biodegradability properties. Natural fibers have found use as reinforcement in composites, in the automotive industry, packaging and in the energy sector. Generally, natural fibers are obtained from plants or animals,[1] and their properties depend on their source, as well as on the extraction, processing and modification methods applied. Natural fibers extracted from plants are called lignocellulosic, as they are constituted of complex structures of cellulose, lignin and hemicelluloses.[2] Before actually using the fibers as reinforcement in a polymer matrix, it is necessary to clean and adjust the surface of the fibers. Various physical, chemical and biological methods are used to treat fibers.

Cellulose is also a renewable natural polymer, which is mainly found in wood and non-wood sources, such as agricultural residues. It is an unbranched polysaccharide with a long chain, which is formed by D-glucopyranose units linked by β-(1,4)-glycosidic bonds. Between the oxygen atoms and the hydroxyl groups of the D-glucopyranose unit, there are intramolecular and intermolecular hydrogen bonds that contribute to the crystallinity of cellulose.[3] Cellulose is characterized by unique properties, such as easy availability, renewability, low weight, and environmental friendliness. In recent years, cellulose has been used as a reinforcing filler in rubber technology. Cellulose has a hydrophilic character due to the presence of hydroxyl groups attached to the D-glucopyranose unit. One of the factors that make it difficult to design polymer composites filled with cellulose is precisely poor interphase adhesion caused by the hydrophobic nature of the rubber matrix and the hydrophilic filler – cellulose. Cellulose is a semicrystalline polymer and due to the presence of surface

hydroxyl groups, it tends to agglomerate. Therefore, it is difficult to prepare a dispersion of hydrophilic cellulose in a hydrophobic matrix of natural rubber. Satisfactory mechanical properties of the prepared composites cannot be achieved by adding pure cellulose as a filler to hydrophobic natural rubber (NR). Therefore, the surface treatment of cellulose is very important.[4,5]

An effective method for improving interphase adhesion is the treatment of cellulose with organosilanes. Organosilanes, such as 3-aminopropyltriethoxysilane (APTES), bis-(3-triethoxysilylpropyl)tetrasulfide (TESPT), 3-isocyanatepropyltriethoxysilane (IPTS), are commonly used to reduce the hydrophilic nature of cellulose. The silane groups are grafted onto the cellulose surface by a chemical reaction between the hydroxyl groups of the cellulose and the end functional group of the silane. The presence of polysulfide bonds in the given silane plays an important role here. Polysulfide bonds have the ability to interact with diene units of the natural rubber matrix.[6,7] Cellulose also exhibits some properties that limit its use in other applications. It is sensitive to moisture, hydrophilic, and has low thermal stability. Methods have been developed for surface treatment of cellulose and pretreatment of cellulose fibres, thereby improving its specific properties in terms of dispersion in nonpolar solvents or polymers. Cellulose can be chemically modified under certain reaction conditions due to the presence of active sites.[8] There are three hydroxyl groups in each cellobiose ring. Secondary (C2 and C3) and primary (C6) groups can be substituted with other functional groups or long chains. The degree of hydroxyl substitution (DS) can be increased by maximizing the available surface area and exposing internal hydroxyl groups, for example, by using swelling agents.[9,10] In recent years, similar reaction mechanisms have been used in studies to introduce silane groups onto the cellulose surface to improve the interfacial adhesion between the hydrophobic matrix and the hydrophilic cellulose filler to modify the mechanical properties of polymer composites.[11]

In this work, we modified cellulose by means of two types of silanes. Modified cellulose was used as a filler for the preparation of composites with a natural rubber matrix. We studied the structural and thermal properties of treated cellulose and NR composites by means of IR spectroscopy, TGA, XRD and SEM microscopy.

EXPERIMENTAL

Materials

Cellulose (CEL) 99.5%, bulk density 90-110 g.cm^{-3} used in this work was provided by Greencel Ltd. Company (Hencovce, Slovakia). Natural rubber SMR 10 (NR) was purchased from Kuala Lumphur Malaysia. For the modification of cellulose, two silanes were used: 3-aminopropyl triethoxysilane (APTES; ≥98%, an aminosilane mostly used in the chemical modification of a variety of surfaces, which can act as an adhesion promoter between polymer and the substrate material, Sigma-Aldrich) and bis-[3-(triethoxysily)lpropyl]-tetrasulfide) (Si69; ≥90%, generally used as a crosslinking agent and reinforcing filler in the manufacturing of rubber, Aldrich). Furthermore, ethanol (96%, mikroCHEM) and glacial acetic acid (99%, AFT) were used.

Cellulose modification

Hydrolysis of silane was performed using an aqueous alcohol solution (ethanol: water = 80:20 v/v) and the silane solution was stirred for 30 min. In the case of APTES, the alcoholic solution was acidified with glacial acetic acid at pH of 4.5 to 5.0. Cellulose was added to the silane solution and the mixture was stirred at room temperature for 2 hours. The silane concentration was 5 wt% according to the content of cellulose. Modified cellulose was filtered, washed twice with 80:20 ethanol/water solution and dried at 105 °C for 48 h. The obtained modified celluloses were denoted as CEL_APTES and CEL_Si69, according to the modifying agent. The work methodology is shown Figure 1.

Preparation of NR composites

Modified cellulose was melt-blended with NR in a Brabender Plasti-Corder PLE 331 (Brabender GmbH & Co. KG, Germany). The mixing was carried out at 80 and 90 °C and 50 rpm. The content of CEL, CEL_APTES or CEL_Si69 was 45 parts per hundred rubbers (phr), respectively. The amount of CEL filler of 45 phr was chosen based on previous research, where the given amount of filler appeared to be optimal in terms of several properties of the prepared composites.[12,13] The composites were vulcanized with the following formula: stearic acid, ZnO, Flavex, N-tert-butyl-2-benzothiazolesulfenamide and sulphur. The temperature of vulcanization was 150 °C.

Characterisation of samples

Infrared spectroscopy

Infrared spectra (IR) of cellulose samples as well as composites were obtained using a Nicolet iS50 FTIR spectrometer (ThermoFisher Scientific, USA), equipped with an ATR diamond accessory. For each absorption spectrum in the region of 4000 to 400 cm^{-1}, 32 scans were obtained with a scan resolution of 4 cm^{-1}.

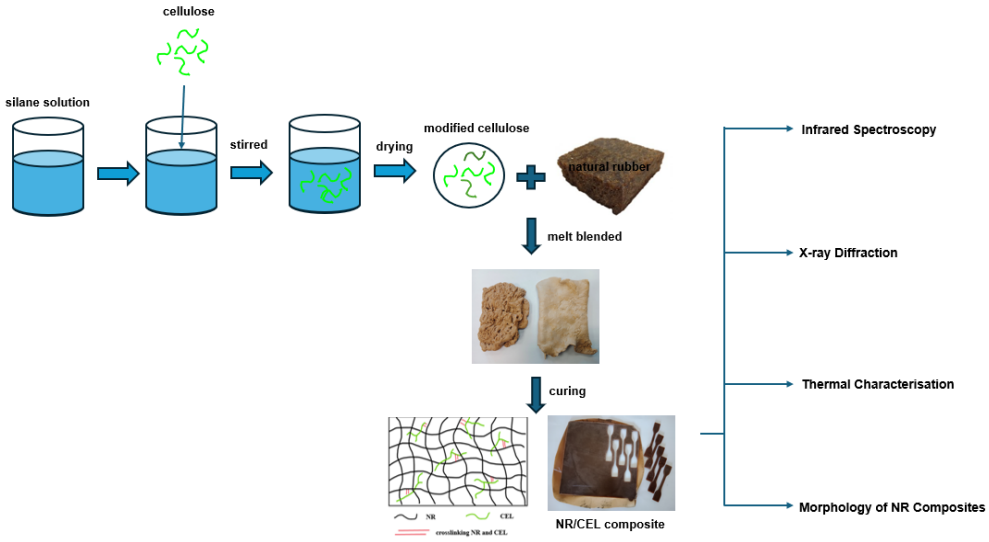

Figure 1: Work methodology

X-ray diffraction

X-ray diffraction (XRD) analysis of cellulose samples was performed using a PANalytical Empyrean X-ray diffractometer (PAN Analytical, the Netherlands), equipped with CuKα radiation (λ = 1.5405 Å). XRD patterns were measured in the 5–45° 2Theta range. The crystallinity index (*CrI*) was calculated based on the empirical Segal equation (1) according to:[14,15]

$$CrI = \frac{(I_{200} - I_{am})}{I_{200}} \times 100 \quad (1)$$

where I_{200} and I_{am} are the intensities of the diffraction peaks that relate the crystalline (200) plane (maximum intensity) and the amorphous part (minimum intensity between 18° and 19° 2Theta).

Thermal characterisation

The thermal properties of the unmodified cellulose and the modified celluloses, as well as the NR composites filled with the given celluloses, were studied using a TGA/DSC2 STARe Mettler Toledo System, at a heating rate 10 °C.min^{-1} in nitrogen atmosphere (gas flow 50 mL.min^{-1}) in the range of 30 to 600 °C. The weight of the cellulose samples was ~10 mg and the weight of composites ranged from 30 to 35 mg.

Morphology of NR composites

For observing the morphology of the samples, all specimens were broken at the temperature of liquid nitrogen and fracture surfaces were coated by an ultrathin layer of gold using high-vacuum evaporation. Micrographs of specimens were taken by the scanning electron microscope VEGA TS 5130 MM (Tescan, Brno, Czech Republic) at the accelerating voltage of 20 kV. All micrographs are backscattered electron (BSE) images.

RESULTS AND DISCUSSION

Characterization of modified cellulose and NR composites

Infrared spectroscopy was used to identify the chemical bonds based on the intensity of absorption peaks of the functional groups. The IR spectra for studied celluloses are shown in Figure 2, and the detected absorption peaks and their assignments according to the literature are summarised in Table 1. The spectra of unmodified and modified celluloses have shown a strong wide band in the spectral region of 3100–3600 cm^{-1} due to the presence of the free O–H stretching vibrations in cellulose.[14-17] The wide peak detected around 2892 cm^{-1} is characteristic of C–H asymmetric and symmetric stretching vibration.[16,17] The peak observed at 1636 cm^{-1} is related to the O–H bending of the adsorbed water. The peak at 1428 cm^{-1} is associated with the bending symmetric vibration of –CH_2, in-plane O–H bending vibration and O–C–H bonding. The peak at 1365 cm^{-1} corresponds to the bending vibration of the C–H and C–O bonds in the polysaccharide aromatic rings.[14,18-22] The peak detected at 1315 cm^{-1} is related to the C–O stretching vibration in ester, bending vibrations of C–H and C–O groups in the rings in polysaccharides and CH_2 wagging vibration.[23,24] The peaks at 1315 and 1334 cm^{-1} are assigned to the bending of hydroxyl group in cellulose. The peaks at 1161 and 1104 cm^{-1} are due to the C–C ring stretching and C–O–C glycosidic ether, respectively. The peak at 1050 cm^{-1} is ascribed to the C–O stretching vibration of cellulose. The sharp peak observed at 1027 cm^{-1} is due to the C–

O–C stretching vibration in the pyranose ring and C–C stretching vibration. This wavenumber is characteristic of cellulose that is hemicellulose and lignin free.[14,16,17,23,24] The peaks in the spectral region of 1165–1025 cm^{-1} can be also attributed to the C–H rocking vibrations of the pyranose ring skeleton. The peak at 896 cm^{-1} is associated with the glycosidic linkages between glucose units in cellulose (related to C–H deformation and C–O–C).[14,15,24]

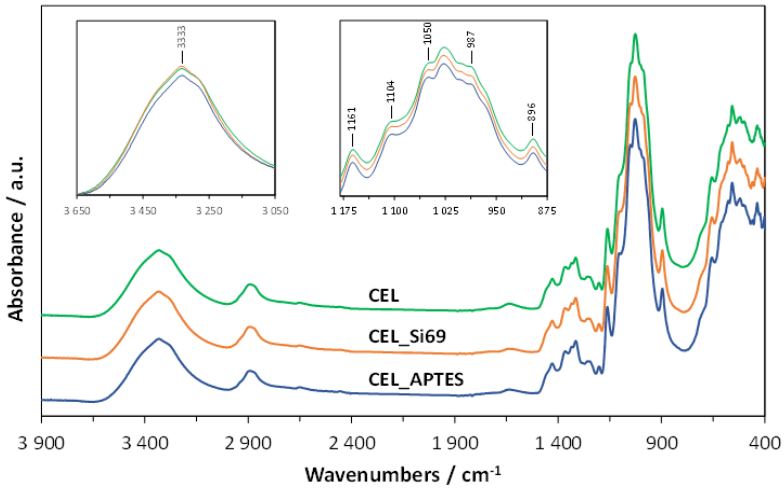

Figure 2: IR spectra of unmodified and modified celluloses

Table 1
Peak positions and assignments in FTIR spectra of unmodified and modified celluloses

Assignments	Peak positions (cm^{-1})			
	CEL	CEL_Si69	CEL_APTES	References
ν(O–H)	3333	3334	3331	14,15
ν(C–H)	2892	2890	2894	16,17
(O–H)	1637	1635	1636	18,19
δ(CH_2)				
β(O–H)	1428	1428	1428	20,14,15,19
O–C–H				
δ(C–H)	1365	1366	1364	16,22
δ(C–O)				20
δ(OH)	1334	1334	1333	15
ν(C–O) / δ(C–H)				18,19
ω(CH_2)	1315	1315	1315	23,24
δ(O–H)				16
τ(CH_2)	1257	1256	1257	16
ν(C–O–C)	1202	1202	1201	16
ν(C–C)	1161	1162	1161	17
ν(C–O)				15
ν(C–O)	1104	1104	1104	16,17
ν(C–C)				18
ν(C–O)	1050	1049	1050	23,24
ν(C–O)	1027	1027	1027	23,24,39
ν(C–C)				18
C–O–C / C–H	896	896	896	23,24,39

Note: ν – stretching, δ – deformation, β – in plane bending, ω – wagging, τ – twisting

After modification of cellulose with both silanes, there were small changes in the intensities of some peaks. For cellulose modified with both silanes, the intensity of the peaks at about 1315, 1161, 1104 and 1050 cm^{-1} was increased, in comparison with those in unmodified cellulose,

and for the peak at about 896 cm^{-1}, was only in the case of the modification with APTES. The IR spectrum of CEL_Si69 is similar to that of CEL. There is no presence of silane characteristic peaks, such as the $–CH_2$ and $–CH_3$ stretching vibrations of Si69 in the spectral range of 2980–2930 cm^{-1}, the C–O–Si bond at about 1238 cm^{-1}, or Si–O–Si stretching vibration of siloxane groups of Si69 at 1037 cm^{-1}.[16,17,23,24] The possible explanation for this is that the concentration of Si69 silane on the cellulose surface is too small to be detected by FTIR, and this agrees with the findings achieved by SEM-EDX and TGA analyses. In the IR spectrum of cellulose modified with APTES, there was a reduction of the intensity of the peaks at 3331, 2894 and 1636 cm^{-1} in comparison with those in the unmodified cellulose. The peak at about 2894 cm^{-1} is characteristic of the C–H stretching vibration. The intensity reduction of the peaks at 3331 and 1636 cm^{-1} for CEL_APTES cellulose can be due to the reduction of hydrogen bonding on the cellulose surface, due to the reaction with the silanol groups from silane.[21,25] However, peaks typical of APTES were not observed in the FTIR spectrum, such as amine groups occurring about at 1565 and 1481 cm^{-1}, N–H bending vibration of primary amine about at 1550 cm^{-1}, or the $Si–CH_3$ bond about at 810 and 749 cm^{-1}. Moreover, the characteristic peaks of Si–O–Si and Si–O–C around at 1135 and 1150 cm^{-1} are difficult to see because they overlap with the intense peak of C–O–C vibration from cellulose in the same spectral region.[14,20,21,25]

Figure 3 shows the IR spectra of NR and NR composites filled with unmodified cellulose (NR/CEL) and modified celluloses (NR/CEL_Si69 and NR/CEL_APTES), and Table 2 summarises the detected absorption peaks and their assignments. In the IR spectra of NR, the broad band with a maximum at about 3295 cm^{-1} is related to the N–H symmetric stretching vibration of proteins.[26,27] In comparison with NR, the bands of NR/CEL, NR/CEL_Si69 and NR/CEL_APTES in the given spectral region are much sharper and stronger (with a maximum about at 3336 cm^{-1}), indicating the presence of adsorbed water and higher densities of the hydroxyl groups in the composites.[16,17] However, in comparison with NR_CEL composite, the intensity of this hydroxyl band is lower for the composites filled with modified celluloses. In the IR spectrum of NR, the peak detected at 3036 cm^{-1} is assigned to the olefin =CH– stretching vibration. There are four dominant peaks in the spectral region of 3300–2800 cm^{-1}. The peaks with maxima at 2960 and 2916 cm^{-1} are assigned to the asymmetric and symmetric stretching vibrations of CH_3. The peak about at 2927 cm^{-1} is assigned to the asymmetric stretching vibration of CH_2. The peak with a maximum at 2851 cm^{-1} corresponds to the symmetric and asymmetric CH_2 stretching vibrations, as well as CH_3 symmetric stretching vibration. The peak at 2726 cm^{-1} relates to the overtone of the CH_2 umbrella vibration and asymmetric CH_3 deformation vibration in NR.[24,25,26]

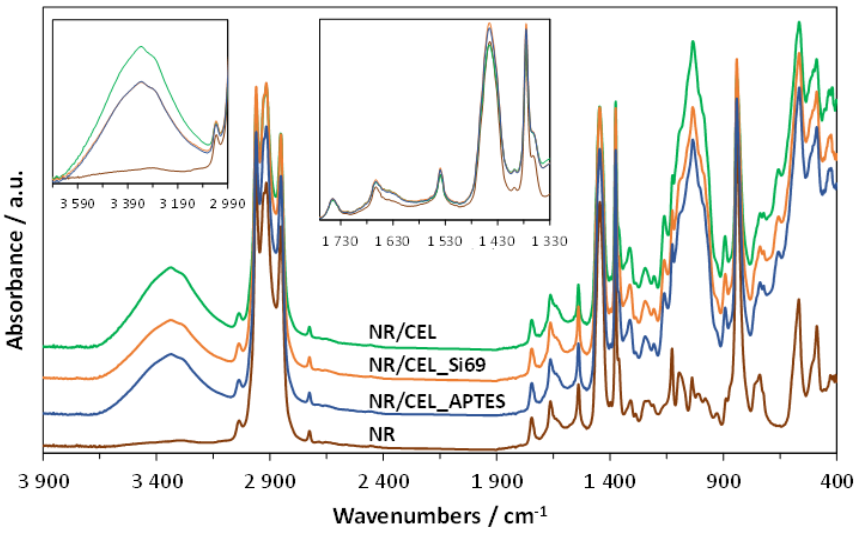

Figure 3: IR spectra for NR and NR composites filled with unmodified and modified celluloses

Table 2
Peak positions and assignments in FTIR spectra of NR and NR composites filled with unmodified cellulose and modified celluloses

Assignment	Peak positions (cm^{-1})				
	NR	NR/CEL	NR/CEL_Si69	NR/CEL_APTES	References
ν(O–H)		3336	3336	3334	16,17
ν(N–H)	3292	~3290	~3290	~3290	26,27
ν(C–H)	3035	3036	3036	3036	26,27
$\nu_{as}(CH_3)$	2960	2960	2960	2960	26,27
$\nu_{as}(CH_2)$	2927	~2926	~2926	~2926	26,27
$\nu_s(CH_3)$	2916	2916	2916	2916	16,17
$\nu(CH_2)/\nu_s(CH_3)$	2851	2852	2851	2851	26,27
$\delta_{as}(CH_3)$	2725	2726	2726	2726	27
$\gamma(CH_2)$					16
ν(C=O)	1745	1745	1745	1745	26,27
ν(C=C)	1663	1663	1663	1663	16,17
δ(O–H)	~1637	~1637	~1637	~1637	16
β(N–H)/ν(C–N)	1540	1540	1540	1540	26,27
$\delta(CH_2)$	1445	1446	1446	1446	16,17
$\delta_{as}(CH_3)$	1376	1375	1375	1375	26,27
$\delta_{as}(CH_3)$	1362	~1362	~1362	~1362	27
δ(C–H)/δ(C–O)					16,17
$\delta_s(CH_3)$	1309	1313	1313	1313	27
ν(C–O)/δ(C–H)					16,17
β(C–H)	1287	1287	1287	1287	27
ν(C–O)/$\tau(CH_2)$	1245	1245	1245	1245	27
ν(O–P–O)	1210	1206*	1207*	1207*	16,17
$\omega(CH_2)$		1161*	1161*	1161*	
ν(C–C)	1127	1125	1125	1125	27
$\omega(CH_2)$					
ν(C–C)	1095				26
$\tau(CH_2)$					
ν(C–C)	1038	1035*	1035*	1035*	16,27
$\rho(CH_3)$					
ν(C–C)	1011				27
τ(C=C)	980				27
ν(C–C)	926				27
$\omega(CH_3)$	888	893*	892*	892*	27
γ(=C–H)	841	841	841	841	26,27
$\rho(CH_3)$					16
$\rho(CH_2)$	740	738	739	738	27
		657*	657*	658*	27
β(C–C)	568	567	566	566	27
β(C–C)	488	489	489	489	27

Note: ν – stretching, δ – deformation, β – in-plane bending, ω – wagging, τ – twisting, γ – out-of-plane bending; ~: shoulder, *: assignment for cellulose (Table 1)

In comparison to NR, the intensity of $\nu_{as}(CH_3)$ peak at 2960 cm^{-1} is decreased for the NR/CEL composite, but for composites filled with modified cellulose it is preserved. In comparison to the composite filled with unmodified cellulose (NR/CEL), the intensities of the CH_3 and CH_2 vibrations in the spectral region of 3000–2800 cm^{-1} increased when the NR was filled with modified cellulose (NR/CEL_Si69 and NR/CEL_APTES).

In the IR spectrum of NR, the peak at 1745 cm^{-1} is characteristic for the C=O bond in phospholipids.[26,27] The peak with a maximum at 1663 cm^{-1} and its wide shoulder about at 1637 cm^{-1} are assigned to the ν(C=C) stretching modes in

cis-1,4-polyisoprene (NR).[16,26,27] In NR composites, the intensity of the mentioned peak increased and, as stated previously,[17] this can also be associated with the δ(O–H) bending modes originating from the cellulose. The peak at 1540 cm^{-1} corresponds to the N–H bending and C–N stretching vibrations in proteins.[26,27] In the spectra of NR as well as NR composites, there are numerous defined peaks in the spectral region of 1500–400 cm^{-1}. The peaks of the CH, CH_2 and CH_3 deformations, and CH_2 twisting modes are dominant for the spectral regions of 1500–1300 cm^{-1} and 1300–1200 cm^{-1}, respectively. The peaks with the highest intensity at 1446 and 1375 cm^{-1} are assigned to $\delta(CH_2)$ and $\delta(CH_3)$ deformations, respectively, which originate from NR.[16,17,26,27] The peaks at ~1360 and 1313 cm^{-1} are assigned to the asymmetric and symmetric $–CH_3$ deformations, respectively. The peak about 1210 cm^{-1} corresponds to the O–P–O asymmetric stretching vibration of phospholipids.[16,17] In the IR spectrum of NR, there are three well defined peaks of the C–C stretching modes at 1127, 1095 and 1038 cm^{-1}.[16,18] The intense peak detected at 841 cm^{-1} is attributed to the out-of-plane =CH bending of cis-1,4-isoprene monomer and the CH_3 rocking mode.[16,17,26,27] In comparison with the NR composite filled with unmodified cellulose, the intensities of the peaks for the $\delta(CH_2)$, $\delta(CH_3)$ and $\rho(CH_3)$ / γ(=C–H) vibrations at 1446, 1375 and 841 cm^{-1}, respectively, in the NR composites filled with modified cellulose was increased. In the spectral region of 1270–870 cm^{-1}, the characteristic peaks originate from cellulose are present in the FTIR spectra of the composites, such as ν(C–O) at about 1060 and 1035 cm^{-1} and ν(C–C) at 1161 cm^{-1}. For NR/CEL_Si69 and NR/CEL_APTES composites, there was observed a reduction of the intensity for the absorption peaks in the region of 1200–900 cm^{-1} in comparison to the NR/CEL composite, but for the peak at 841 cm^{-1}, the intensity increased. There is no significant difference between the spectra of the composites filled with cellulose modified by Si69 and APTES.

XRD analysis of modified and unmodified cellulose

X-ray diffraction was used to get an insight into the crystalline structure and crystallographic phases of unmodified cellulose and modified celluloses. The X-ray diffractograms of the studied celluloses are shown in Figure 4. Modified and unmodified celluloses showed typical cellulose I structure, with peaks around 15.9°, 22.4° and 34.5° of 2Theta.[15,21] The same position of the peaks for the modified celluloses indicates that the process of modification influenced mainly the cellulose surface.[14] This statement will be also be confirmed later through SEM analysis. After modification with the silanes, the intensity of the diffraction peaks at 15.9° (110 plane) and 22.4° (200 plane) was enhanced. The crystallinity index value of CEL, CEL_Si69 and CEL_APTES was calculated to be 58.9%, 65.4% and 65.7%, respectively. These results indicate that unmodified cellulose was less crystalline than the silane-modified celluloses. It can be suggested that, during the modification with the given silanes, a part of the amorphous components of cellulose were removed.

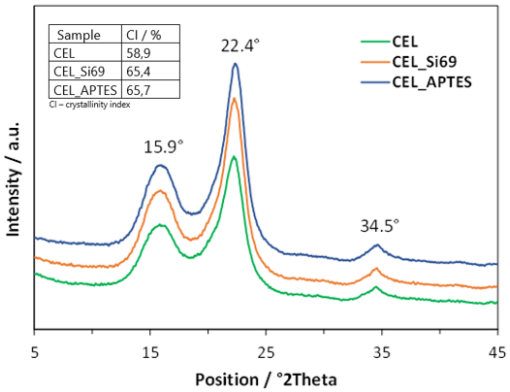

Figure 4: X-ray diffractograms of unmodified cellulose (CEL) and modified celluloses (CEL_Si69 and CEL_APTES)

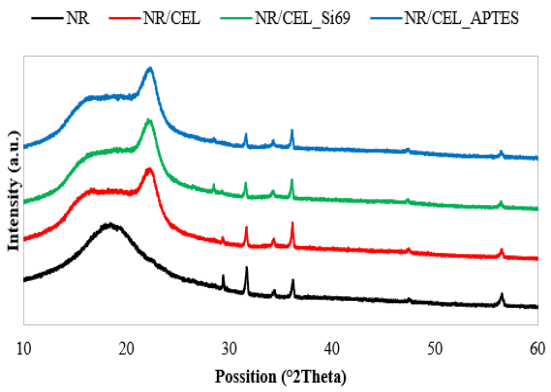

Figure 5: X-ray diffractograms of NR and NR composites filled with unmodified cellulose (NR/CEL) and modified celluloses (NR/CEL_Si69 and NR/CEL_APTES)

The crystallinity index value of cellulose (CEL) used in the work is lower than the value of 73.91% for commercial cellulose isolated from wood pulp, or for cellulose microfibers isolated using different methods from different sources, such as wheat straw (77.8%), soybean husks (69.6%), sisal fibers (75%), agave fibers (64.4%).[28]

In Figure 5, the XRD diffractograms of the unfilled NR and the prepared NR composites filled with unmodified and modified celluloses are shown. In the case of the unfilled NR, it is possible to observe a diffusion band around 18° wide, typical of amorphous natural rubber. Sharp peaks belonging to ZnO, and stearic acid are observed in the region of 30° to the right. For NR composites filled with cellulose and modified cellulose, a change in the intensity of the wide peak at 19.9° can be observed.[29] The characteristic peaks at 22.4°, typical of cellulose, indicate an insufficient dispersion of the filler in the NR matrix. These observations are in good agreement with the SEM study of cellulose-filled NR composites.

Thermal properties of silane modified cellulose and NR composites

Thermogravimetric analysis (TGA) is a widely used method for analysis of thermal decomposition of fillers as well as polymers. Results from TG analysis show the mass loss of substances in relation to temperature change of thermal degradation and the first derivative of TG curve (DTG) shows the corresponding rate of mass loss. The maximum peak of this DTG curve, expressed as temperature of thermal decomposition, can be used for comparison of thermal stability of different materials.[14,30] The TG and DTG curves obtained at a heating rate of 10 °C.min^{-1} for the unmodified cellulose and cellulose modified with APTES and Si69 are shown in Figure 6.

The degradation profile of unmodified and modified celluloses is the same, and it means that the silanization did not affect the thermal degradation process of the studied cellulose, which agrees with the literature.[21,30] The TG curve of the unmodified cellulose and silane-modified celluloses (Fig. 6) displays two mass loss stages.[13,14,21,31] In the temperature region up to 115 °C, the first step with a small mass loss (3.5% and 3.6% for the unmodified cellulose and celluloses modified with silanes, respectively) is related to the vaporization of water and other low molecular weight components present in the cellulose. The second step from 300 °C to 400 °C is assigned to the decomposition of cellulose due to the depolymerization of cellulose chains. Thermal data obtained from TG/DTG/DSC curves for unmodified cellulose and for the silane-modified celluloses are summarised in Table 3.

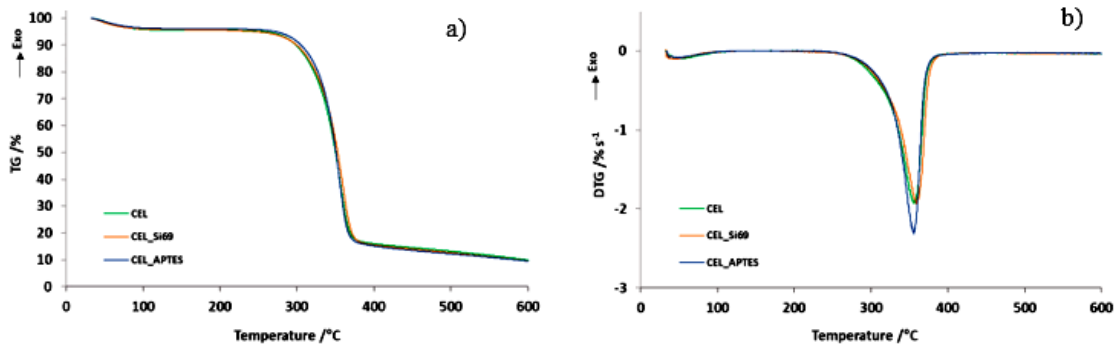

Figure 6: TG (a) and DTG curves (b) of unmodified cellulose (CEL) and modified celluloses (CEL_Si69, CEL_APTES)

Table 3
Thermal data from TG/DTG/DSC curves

Sample	Δm, %		2nd step		
	1st step	2nd step	T_{onset}, °C	T_m, °C	ΔH, J.g^{-1}
CEL	3.5	86.5	327.7	358.9	-177.9
CEL_Si69	3.6	86.6	330.5	359.6	-173.3
CEL_APTES	3.6	87.0	331.5	355.5	-210.5

The T_{onset} was 327.7, 330.5 and 331.5 °C for CEL, CEL_Si69 and CEL_APTES samples, respectively. In comparison with the unmodified cellulose, the modification with silanes leads to an increase in T_{onset} by ~3 °C for cellulose modified with APTES and by ~2 °C for cellulose modified with Si69. The temperature at the maximum degradation rate (T_{max}) for the cellulose modified with APTES is lower by 3.5 °C in comparison with the unmodified cellulose. The given result indicates a slight decrease in the thermal stability of cellulose after the APTES treatment. T_{max} for the cellulose modified with Si69 silane is higher by 0.7 °C compared to the unmodified cellulose. The effect of silanization using Si69 silane on the thermal stability of cellulose is negligible. According to a previous study,[32] the T_{max} of cellulose modified with Si69 is lower by 5 °C than that of unmodified cellulose, *i.e.*, the modified cellulose has a slightly lower thermal stability. The degradation temperature depends on the functional group attached to the microcrystalline cellulose.[33] In another study,[34] the authors have associated the reduction in thermal stability of cellulose after the chemical modification to the reducing ends of the cellulose chain, whose C–OH bonds can form aldehyde groups that are susceptible to oxidation and reduction reactions. Since the silanization process with APTES took place in an acidic environment (pH 4–5), some breakage of β-(1–4) glycosidic bonds may occur, creating more reducing ends. The reduced cellulose chains then decompose more easily than the original cellulose chain. Other researchers[21] related the thermal stability of chemically modified cellulose to the crystallinity rather than to chain ends. According to R. Motta *et al*.,[21] the reduction in thermal stability is related to the higher crystallinity of cellulose and the difficulties of heat transfer, which leads to more thermally labile bonds. This finding is also supported by the results of the XRD analysis of the studied samples. The decrease of T_{max} after the silanization process can be due to the functionalization process, where –OH groups are replaced by the silane-coupling agent.[31]

The thermal behaviour of unmodified and silane-modified celluloses was monitored by DSC analysis (Fig. 7). The values of enthalpy change assigned to the decomposition of the unmodified and the silane-modified celluloses are shown in Table 3. The DSC profile of the studied cellulose showed an obvious and big endothermic peak at 359 °C. Thermal decomposition of cellulose in N_2 atmosphere is an endothermic process.[32] The enthalpy change value assigned to the decomposition of the cellulose modified with APTES is lower than the enthalpy change value for the unmodified cellulose. In the case of the cellulose modified with Si69, the enthalpy change value is identical to that of the unmodified cellulose. TGA analysis can be also used to determine the amount of silane grafted onto the surface of cellulose by correlating the final residue of the neat and grafted (modified) samples up to 380 °C.[33,34] From the difference in the mass loss (%) under nitrogen atmosphere within the 150–380 °C temperature range (Fig. 6), it is possible to calculate the quantity of grafted silane molecules onto the surface of cellulose. This can be achieved according to the following Equations (2) and (3):[33]

$$\text{Amount of silane grafting } (\text{mg.g}^{-1}) = 1000.W_{150-380} \quad (2)$$

$$\text{Amount of silane grafting } (\text{mg.mol}^{-1}) = \frac{\text{Amount of silane grafting}}{M} \quad (3)$$

where $W_{150-380}$ is the difference between the normalized weights of samples at 105 °C and 380 °C, M is the molecular weight of the grafted silane molecules ($g.mol^{-1}$). The molecular weight of APTES and Si69 is 221.37 and 538.95 $g.mol^{-1}$, respectively.

The $W_{150-380}$ (%) values and the grafted silane quantity in $mg.g^{-1}$ and $mmol.g^{-1}$ of cellulose, calculated from the TGA under nitrogen, are presented in Table 4.

It can be seen that, in the case of both silanes, the amount of grafted silane is significantly lower than previous results reported in the literature.[33,34] In the case of cellulose modified with APTES, the grafted amount of silane is higher compared to that obtained for cellulose modified with Si69, and it can be attributed to the presence of the high polar amino end group (NH_2) in APTES, which favoured the interaction between the APTES and the cellulose, driven by the formation of hydrogen bonds.[35] The concentration of APTES in the modification solution influences the quantity of amino silanes able to bond with cellulose.[21,25,33] The increase of grafting with the silane amount can also be attributed to the steric hindrance and low concentration of –OH groups on the particle surface.[36] The result concerning the APTES was confirmed by FTIR data. We can conclude that the amount of grafted Si69 silane onto the surface of cellulose is very small and the silanization

process with Si69 has a negligible influence on the thermal stability of cellulose. The amount of grafted silane APTES to the surface of cellulose is higher and the silanization process slightly reduced the thermal stability of the modified cellulose.

The thermal properties of natural rubber (NR) and NR composites filled with unmodified cellulose (NR/CELL) and cellulose modified with silanes (NR/CEL_Si69 and NR/CEL_APTES), were investigated using TG analysis. Figure 8 shows the TG and DTG curves of NR and NR composites filled with cellulose and modified celluloses.

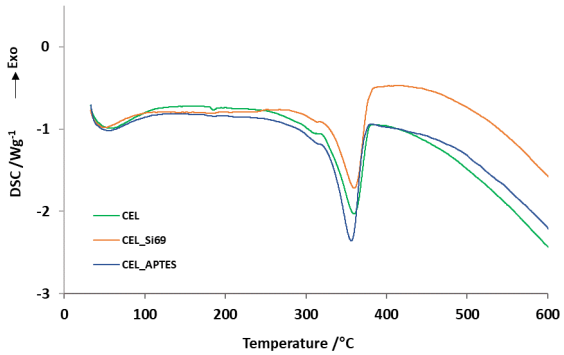

Figure 7: DSC curves of unmodified cellulose (CEL) and modified celluloses (CEL_Si69, CEL_APTES)

Table 4
$W_{150-380}$ values and grafted silane content in composites, obtained from TGA

Sample	$W_{150-380}$, %	Grafted silane	
		mg.g^{-1}	mmol.g^{-1}
CEL_Si69	0.7	7.1	0.013
CEL_APTES	1.5	15	0.068

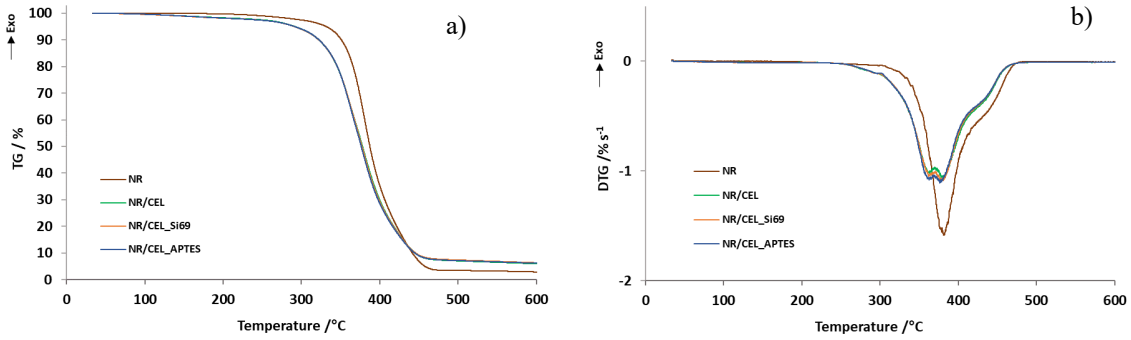

Figure 8: TG (a) and DTG curves (b) of NR and composites NR/CELL, NR/CEL_Si69 and NR/CEL_APTES

TG and DTG curves of NR (Fig. 8) exhibit two stages of decomposition, and the thermal degradation takes place between 290 and 470 °C. The first stage of decomposition is in the range of temperatures of 290–410 °C, and corresponds to the decomposition of double bonds of methylene groups in polyisoprene molecules, *i.e.*, to the decomposition of natural rubber. The second stage, in the temperature range from 410 to 470 °C, can be assigned to the carbonization of natural rubber. The total mass loss of natural rubber is 95.1%.

TG and DTG curves of the composites filled with unmodified cellulose (NR/CEL) and composites filled with silane-modified celluloses (Fig. 8) exhibit three stages of decomposition.[12,13] The degradation of all composites with the cellulose filler takes place in the temperature range of 260 to 460 °C. The first stage occurs in the temperature range of 260–385 °C and belongs to the decomposition of cellulose. The second stage of decomposition occurs in the range of

340–410 °C and corresponds to the decomposition of natural rubber. The third stage occurs in the temperature range of 410–460 °C and corresponds to the carbonization of the rubber. For all filled composites, the total mass loss is ~90.5%. After the thermal degradation of NR composites filled with cellulose, there is a higher residue due to the products of thermal decomposition of cellulose. All filled NR composites show a lower initial temperature of degradation compared to the NR. From the DTG (Fig. 8b)) curve, it can be seen that the thermal stability of NR composites (NR/CEL, NR/CEL_Si69 and NR/CEL_APTES) is almost the same, and silanization of cellulose has a negligible effect on the thermal stability of composites. The temperature of peak maximum and the enthalpy change value of processes were evaluated from DSC curves of the NR and composites filled with unmodified and modified celluloses (Fig. 9), and the obtained characteristics are summarised in Table 5.

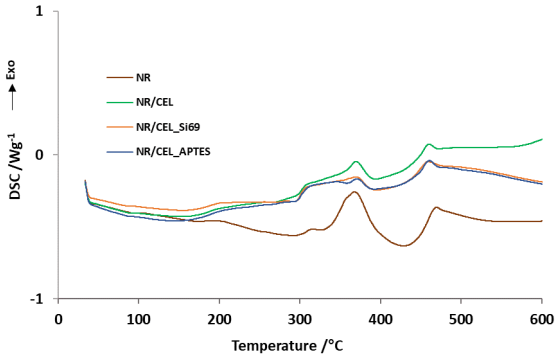

Figure 9: DSC curves of NR and NR/CELL, NR/CEL_Si69 and NR/CEL_APTES composites

Table 2
Characteristics of processes obtained from DSC curves of NR and NR composites

Sample	Effect I		Effect II		Effect III	
	T_m, °C	ΔH_I, J.g^{-1}	T_m, °C	ΔH_{II}, J.g^{-1}	T_m, °C	ΔH_{III}, J.g^{-1}
NR	-	-	369.5	14.3	467.8	17.2
NR/CEL	295.9	-3.7	370.4	9.9	459.1	3.4
NR/CEL_Si69	296.3	-2.1	371.7	3.1	458.8	4.4
NR/CEL_APTES	294.9	-4.7	372.3	2.5	459.8	3.4

DSC curves of NR composites represent "multi-peak" curves due to the fact that the composites were prepared from natural rubber, filler (cellulose) and vulcanizing agents. In DSC curves, the first endothermic peak corresponds to the decomposition of cellulose.[32] The temperature of peak maximum for this endothermic peak is 296 °C in the case of NR/CEL and NR/CEL_Si69 composites, and 295 °C for NR/CEL_APTES composite. In comparison with the composite filled with unmodified cellulose, the value of enthalpy change, which concerns the cellulose decomposition, is gently higher for composite NR/CEL_Si69, while for composite NR/CEL_APTES, this value is lower. The exothermic processes corresponding to the decomposition and the carbonization of natural rubber are other effects in DSC curves.[37,38,39] The temperature of natural rubber decomposition for the NR and NR composite filled with unmodified cellulose is 370 °C. The temperature of decomposition of natural rubber for NR composites filled with cellulose modified by silanes is ~372 °C. The enthalpy change value of decomposition is ~14 J.g^{-1} for NR. In comparison with NR, the enthalpy change value of natural rubber decomposition (ΔH_{II}) decreases by ~4 and ~11 J.g^{-1} for NR composites filled with unmodified cellulose and cellulose modified with silanes, respectively. For NR, the temperature of the natural rubber carbonization is ~470 °C and the enthalpy change value (ΔH_{III}) is 17 J.g^{-1}. For NR composites filled with unmodified and modified cellulose, the values of the carbonization temperature and ΔH_{III} are similar (~460 °C and ~4 J.g^{-1}, respectively), and they were considerably decreased in comparison with those of the NR

sample. For NR composites, no significant influence of cellulose modification with the silanes on the ΔH_I, ΔH_{II} and ΔH_{III} values was observed.

Morphology of modified cellulose and NR composites

Scanning electron microscopy was used to study the effect of cellulose surface modification and its morphology. Figure 10 presents SEM images of the surface morphology of unmodified cellulose and cellulose modified with silanes. As can be seen in Figure 10 (c), the fiber diameter of APTES silane-modified cellulose (CEL_APTES) is smaller than that of unmodified cellulose (CEL). SEM micrographs of modified cellulose fibers appear to be smoother, whereas the surface of unmodified cellulose is slightly scaly.

Figure 11 presents SEM images of unfilled NR, NR composite filled with 45 phr unmodified cellulose (NR/CEL) and NR composites filled with modified cellulose NR/CEL_Si69, respectively. NR/CEL_APTES. The dispersed cellulose phase in the natural rubber matrix indicates a low quality of interface adhesion. The adhesion between filler and matrix is based on intermolecular interactions at the interface. The strain at the interface can be explained by the hydrophilic nature of cellulose and the hydrophobic nature of the natural rubber matrix.[22,38] The cellulose fibers present in the prepared NR composites are randomly oriented and distributed throughout the rubber matrix.

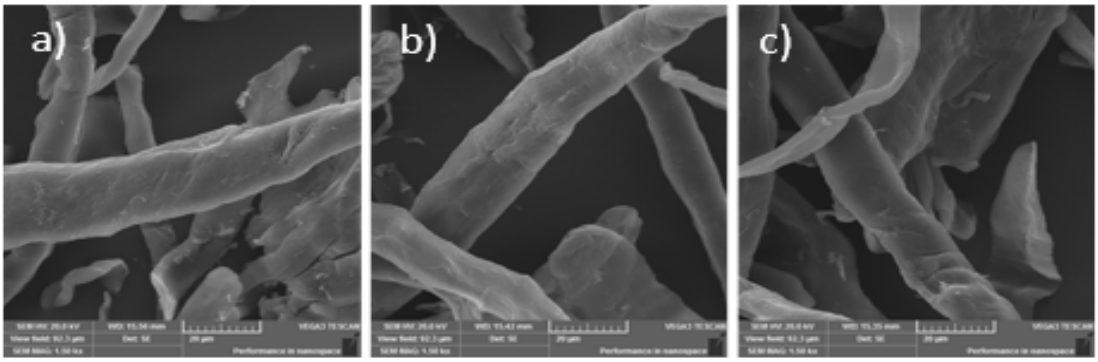

Figure 10: SEM images of unmodified cellulose (a), modified cellulose CEL_Si69 (b) and CEL_APTES (c) at 200x

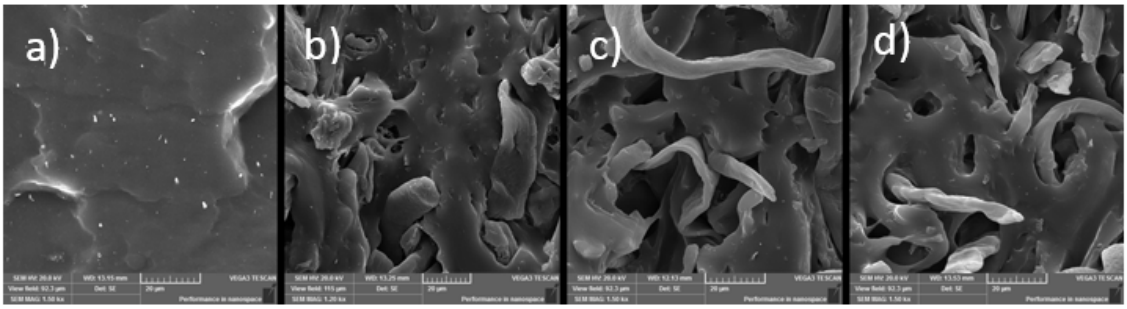

Figure 11: SEM images of unfilled NR (a) and NR/45 phr CEL (b), NR/45 phr CEL_Si69 (c), NR/45 phr CEL_APTES (d) composites at 200x

CONCLUSION

In this work, we used a simple, environmentally friendly method of treating the surface of cellulose microfibers using silylation, without the use of organic solvents. Structure and chemical analyses of the modified celluloses were performed using advanced characterization techniques. SEM showed that the modification did not significantly affect the morphology of the cellulose surface. The effectiveness of the modification was confirmed by ATR-FTIR and XRD. The results showed that the crystalline structure of the celluloses modified by the two silanes was preserved, and modification occurred

mainly on the CEL surface, which confirms the recorded crystallinity index of 58.9% and 65.7% for pure and modified CEL, respectively. The composites of natural rubber (NR) with cellulose and modified celluloses were prepared, which were dosed into the NR matrix in an amount of 45 phr. TG and DSC confirmed that the silanization process has a negligible effect on the thermal stability of cellulose. TG analysis showed a slight decrease in the thermal stability of modified CEL and NR composites filled with 45 phr of modified cellulose by silanes, too. With the mentioned method, the modification of the cellulose surface can be achieved without the need to change solvents. Cellulose modified in this way can be used in the preparation of composites or nano-absorbents. Regarding the modified cellulose, our further studies will be focused on the study of the rheological characteristics, physico-mechanical properties and relationships between the components of the prepared NR/CEL composites.

ACKNOWLEDGEMENTS: This research work has been supported by the Operational Program Integrated Infrastructure, co-financed by the European Regional Development Fund by the project: Advancement and support of R&D for "Centre for Diagnostics and Quality Testing of Materials" in the domains of the RIS3 SK specialization, Acronym: CEDITEK II, ITMS2014+ code 313011W442 and Scientific Grant Agency VEGA 1/0265/24.

REFERENCES

[1] D. Divya, I. Jenish and S. Raja, *Adv. Mater. Sci. Eng.*, **2022**, 12 (2022), https://doi.org/10.1155/2022/8099500
[2] P. Senthamaraikannan and M. Kathiresan, *Carbohyd. Polym.*, **15**, 186 (2018), https://doi.org/10.1016/j.carbpol.2018.01.072
[3] S. F. Kabir, A. Rahman, F. Yeasmin, S. Sultana, R.A. Masud *et al.*, in "Radiation-Processed Polysaccharides", Elsevier, Amsterdam, the Netherlands, 2022, https://doi.org/10.1016/b978-0-323-85672-0.00005-2
[4] D. Klemm, B. Heublein, H. P. Fink and A. Bohn, *Angew. Chem. Int. Ed.*, **44**, 358 (2005), https://doi.org/10.1002/anie.200460587
[5] R. V. Gadhave, P. V. Dhawale and C. S. Sorate, *J. Polym. Chem.*, **11**, 11 (2021), https://doi.org/10.4236/ojpchem.2021.112002
[6] A. Dufresne, in "Encyclopedia of Nanoscience and Nanotechnology", edited by H. S. Nalwa, American Scientific Publishers, 2009, vol. 10
[7] C. Miao and W. Hamad, *Cellulose*, **20**, 20 (2013), https://doi.org/10.1007/s10570-013-0007-3
[8] F. Tao, H. Song and L. Chou, *Bioresour. Technol.*, **102**, 12 (2011), https://doi.org/10.1016/j.biortech.2011.06.067
[9] J. Crawshaw, W. Bras, G. R. Mant and R. E. Cameron, *J. Appl. Polym. Sci.*, **83**, 345 (2002), https://doi.org/10.1002/app.2287
[10] J. Lazko, T. Sénéchal, N. Landercy, L. Dangreau, J. M. Raquez *et al.*, *Cellulose*, **21**, 45 (2014), https://doi.org/10.1007/s10570-014-0417-x
[11] A. Samir, F. Alloin and A. Dufresne, *Biomacromolecules*, **6**, 2 (2005), https://doi.org/10.1021/bm0493685
[12] P. Skalková, I. Papučová, I. Labaj, J. Pagáčová, D. Ondrušová *et al.*, *Mat. Methods Technol.*, **16**, 4, (2022)
[13] I. Papučová, P. Skalková, I. Labaj, J. Pagáčová, M. Pajtášová *et al.*, *Mat. Methods Technol.*, **16**, 13 (2022)
[14] H. Khanjanzadeh, R. Behrooz, N. Bahramifar, W. Gindl-Altmutter, M. Bacher *et al.*, *Int. J. Biol. Macromol.*, **106** (2018), https://doi.org/10.1016/j.ijbiomac.2017.08.136
[15] U. Moonart and S. Utara, *Cellulose*, **26**, 47 (2019), https://doi.org/10.1007/s10570-019-02611-w
[16] F. Agrebi, N. Ghorbel, S. Bresson, O. Abbas and A. Kallel, *Polym. Compos.*, **40**, 11 (2019), https://doi.org/10.1002/pc.24989
[17] A. R. Nair, S. Sambhudevan and B. Shankar, *Cellulose Chem. Technol.*, **53**, 263 (2019), https://doi.org/10.35812/CelluloseChemTechnol.2019.53.26
[18] E. Abraham, B. Deepa, L. A. Pothan, M. John, S. S. Narine *et al.*, *Cellulose*, **20**, 20 (2013), https://doi.org/10.1007/s10570-012-9830-1
[19] J. Lu, P. Askeland and L. T. Drzal, *Polymer*, **49**, 14 (2008), https://doi.org/10.1016/j.polymer.2008.01.028
[20] E. Indarti, R. Rohaizu and W. D. Wanrosli, *Int. J. Biol. Macromol.*, **135**, 34 (2019), https://doi.org/10.1016/j.ijbiomac.2019.05.161
[21] R. Motta, H. L. Ornaghi, A. J. Zattera and S. Campos, *Carbohyd. Polym.*, **230**, 115595 (2020), https://doi.org/10.1016/j.carbpol.2019.115595
[22] N. Lopattananon, D. Jitkalong and M. Seadan, *J. Appl. Polym. Sci.*, **120**, 3242 (2011), https://doi.org/10.1002/app.33374
[23] K. S. M. Rahimi, R. J. Brown, T. Tsuzuki and T. J. Rainey, *Adv. Nat. Sci.*, **7**, 35004 (2016), https://doi.org/10.1088/2043-6262/7/3/035004
[24] L. Srisuwan, K. Jarukumjorn and N. Suppakarn. *Adv. Mater. Sci. Eng.*, **2018**, 45839 (2018), https://doi.org/10.1155/2018/4583974
[25] E. Robles, L. Csóka and J. Labidi, *Coatings*, **8**, 139 (2018), https://doi.org/10.3390/coatings8040139
[26] L. Xu, J. Zheng, C. Huang, M. Luo, W. Qu *et al.*, *RSC Adv.*, **5** (2015), https://doi.org/10.1039/C5RA07428B
[27] S. Rolere, S. Liengprayoon, L. Vaysse, J. Sainte-Beuv and F. Bonfils, *Polym. Test.*, **43** (2015), https://doi.org/10.1016/j.polymertesting.2015.02.011
[28] A. Khenblouche, D. Bechki, M. Gouamid, K. Charradi, L. Segni *et al.*, *Polímeros*, **29**, (2019),

https://doi.org/10.1590/0104-1428.05218
[29] S. Shiva, L. Gopal, B. Dhakar, P. Kapgate, M. Chhajed *et al*., *Polym. Adv. Technol*., **31** (2020), https://doi.org/10.1002/pat.5030
[30] A. Tejado, C. Pena, J. Labidi, J. M. Echeverria and I. Mondragon, *Bioresour. Technol*., **98**, 23 (2007), https://doi.org/10.1016/j.biortech.2006.05.042
[31] W. Bessa, D. Trache, M. Derradji, B. Bentoumi, A. F. Tarchoun *et al*., *Int. J. Biol. Macromol*., **180** (2021), https://doi.org/10.1016/j.ijbiomac.2021.03.080
[32] O. Somseemee, P. Sae-Oui and C. Siriwong, *Ind. Crop. Prod*., **171**, 113 (2021), https://doi.org/10.1016/j.indcrop.2021.113881
[33] D. O. De Castro, J. Bras, A. Gandin and N. Belgacem, *Carbohyd. Polym*., **137**, 1 (2016), https://doi.org/10.1016/j.carbpol.2015.09.101
[34] M. B. Agustin, F. Nakatsubo and H. Yano, *Cellulose*, **23**, 1 (2015), https://doi.org/10.1007/s10570-015-0813-x
[35] M. Abdelmouleh, S. Boufi, M. N. Belgacem, A. P. Duarte, A. Ben Salah *et al*., *Int. J. Adhes. Adhes*., **24**, 1 (2004), https://doi.org/10.1016/S0143-7496(03)00099-X
[36] M. Sabzi, S. M. Mirabedini, J. Zohuriaan-Mehr and M. Atai, *Progress Org. Coat*., **65**, 2 (2009), https://doi.org/10.1016/j.porgcoat.2008.11.006
[37] J. Bras, M. L. Hassan, C. Bruzesse, E. A. Hassan, N. A. El-Wakil *et al*., *Ind. Crop. Prod*., **32**, 3 (2010), https://doi.org/10.1016/j.indcrop.2010.07.018
[38] D. Loof, M. Hiller, H. Oschkinat and K. Koschek, *Materials*, **9**, 6 (2016), https://doi.org/10.3390/ma9060415
[39] S. Y. Oh, D. I. Yoo, Y. Shin and G. Seo, *Carbohydr. Res*. **340**, 17 (2005), https://doi.org/10.1016/j.carres.2004.11.027